

PAPER • OPEN ACCESS

Design Aspects of the Emittance Diagnostic for the Scorpius Accelerator

To cite this article: M.L. Raphaelian *et al* 2024 *J. Phys.: Conf. Ser.* **2687** 072011

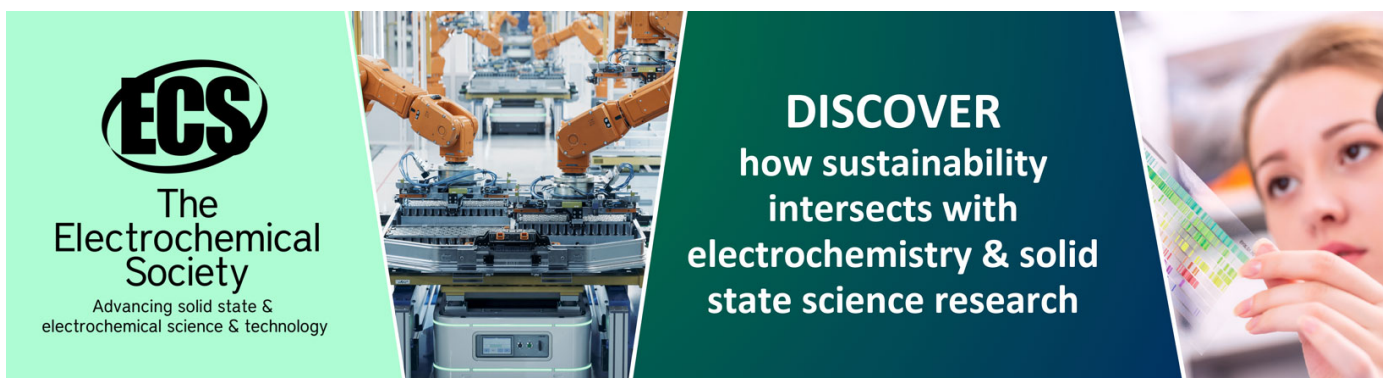
View the [article online](#) for updates and enhancements.

You may also like

- [EVIDENCE FOR EVOLUTION AMONG PRIMORDIAL DISKS IN THE 5 Myr OLD UPPER SCORPIUS OB ASSOCIATION](#)
S. E. Dahm

- [SPITZER SPECTROSCOPY OF CIRCUMSTELLAR DISKS IN THE 5 Myr OLD UPPER SCORPIUS OB ASSOCIATION](#)
S. E. Dahm and John M. Carpenter

- [A CORRELATION BETWEEN CIRCUMSTELLAR DISKS AND ROTATION IN THE UPPER SCORPIUS OB ASSOCIATION](#)
S. E. Dahm, Catherine L. Slesnick and R. J. White



ECS
The
Electrochemical
Society
Advancing solid state &
electrochemical science & technology

DISCOVER
how sustainability
intersects with
electrochemistry & solid
state science research

Design Aspects of the Emittance Diagnostic for the Scorpius Accelerator

M.L. Raphaelian¹, D.M. Dzenitis¹, S.T. Littleton¹, A.A. Mazotti¹, F.A. Weber¹,
N.J. Pogue², P. Duffy², S. Falabella², and W.D. Stem²

¹ Nevada National Security Site, Livermore CA 94550 USA

² Lawrence Livermore National Laboratory, Livermore CA 94550 USA

raphaeml@nv.doe.gov

Abstract. A multi-pulse linear induction accelerator, Scorpius, will be constructed at the NNSS U1A facility for use in radiographic experiments. One of the many diagnostics, the injector emittance diagnostic, will provide information on the quality of the beam emanating from the injector and therefore the quality of the beam in the accelerator. A slit-harp design was chosen for the emittance diagnostic. We have modeled the performance of the diagnostic for various simulated Scorpius beams, using several computational tools depending on the physics of the effects under investigation. Additional modeling of electron stopping power, energy deposition, heat dissipation, and x-ray attenuation drove material choices for the collimator jaws and harp wires. The signal chain is designed around constraints of signal extraction, biasing to suppress crosstalk between harp wires via secondary electron emission, and multi-pulse record capability. The ensemble of materials, electrical, and mechanical aspects of the design to reconstruct the emittance from the injector of the accelerator are described.

1. Introduction

The United States Defense Laboratories: Lawrence Livermore National Laboratory (LLNL), Los Alamos National Laboratory (LANL), and Sandia National Laboratory (SNL), in conjunction with the Nevada National Security Site (NNSS) are building a 22 MeV multi-pulse linear induction electron beam accelerator, Scorpius, for use in subcritical experiments that occur at the NNSS U1A facility. Different teams within each organization are involved with the design and development of one or more of the accelerator elements. This paper describes the Scorpius slit-harp emittance diagnostic design approach from a joint team effort by NNSS Livermore Operations (NNSS/LO) and LLNL

2. Slit-Harp Diagnostic Modeling

The slit-harp emittance diagnostic is composed of two distinct subsystems. The first is the slit and the second is the harp. The slit is used to select the position within the (vertical) beam profile and the harp is used to measure the transverse momentum components at that position [1-3].

A model of the slit-harp emittance diagnostic was created in COMSOL, a Multiphysics simulation software package. The model consisted of an electron source, a slit, and a detector plane representing the harp (figure 1). LLNL provided beam tunes as the input to the simulations. Each input beam file contains 25,000 macro-particles, each with its position and momentum given by an LLNL injector simulation up to a designated handoff point.



In each simulation, the electrons propagate from the source to the slit jaws, with the slit center offset by x_S . The electrons that are not stopped by the jaws propagate to the detector plane, where their position, x_H , is recorded.

Each jaw consists of a rectangular block of height h and overall thickness d_{bulk} , with a tapered section near the aperture that reduces the thickness to the collimation depth d at the aperture.

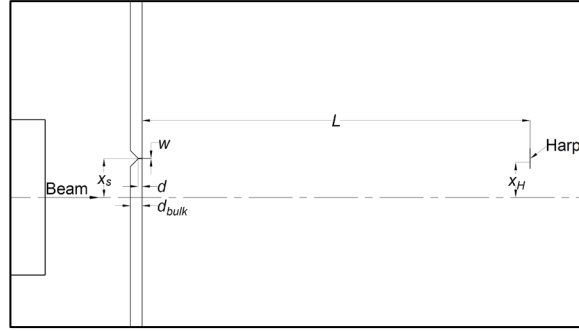


Figure 1: Schematic representation of the geometry used in simulating the slit-harp diagnostic and emittance reconstruction performance. For illustrative purposes, x_H is labeled for an arbitrary harp wire.

2.1. Emittance Reconstruction

An entire emittance reconstruction procedure consists of a series of single simulation runs at different offsets x_S spanning the beam diameter at the jaws (± 44 mm) for a single aperture width w and collimation depth d . We analyzed the quality of phase space reconstruction results across different aperture widths w ($100 \mu\text{m} \leq w \leq 4,000 \mu\text{m}$), collimation depths d ($1 \text{ mm} \leq d \leq 2 \text{ mm}$), and beam tunes ($1.7 \text{ MeV} \leq E \leq 2.0 \text{ MeV}$).

To reconstruct the emittance, each wire is given a x and x' value associated with the center of the wire and the slit offset. The electrons within the bins that make up the wire contribute to the expected signal in the respective wire. For emittance reconstruction, all the signal data across all offsets for a given aperture width w and collimation depth d are analyzed using the equation

$$\tilde{\epsilon} = \sqrt{\overline{x^2 x'^2} - \overline{xx'}^2},$$

where the overbar denotes an average over the signals on all wires for all offsets, e.g.

$$\overline{x^2} = \frac{\sum_{x,x'} I(x,x')(x - \bar{x})^2}{\sum_{x,x'} I(x,x')},$$

and $I(x,x')$ is the signal on the harp wire at $x_H = x_S + x'L$ with slit offset $x_S = x$. This can be the integrated signal over the beam pulse duration or the instantaneous signal. The instantaneous signal will enable measurement of the evolution of the beam phase space during the pulse.

Using the above methodology, we simulated emittance reconstruction for a variety of slit widths, harp wire diameters, and wire spacings. The results indicate that a jaw design with an aperture width of $100 - 200 \mu\text{m}$ and a collimation length of 2.0 mm , coupled with a harp design with 21 harp wires, a wire diameter of $250 \mu\text{m}$, and separation of $500 \mu\text{m}$, should enable reliable measurement of the Scorpius beam within several percent of the true value (figure 2).

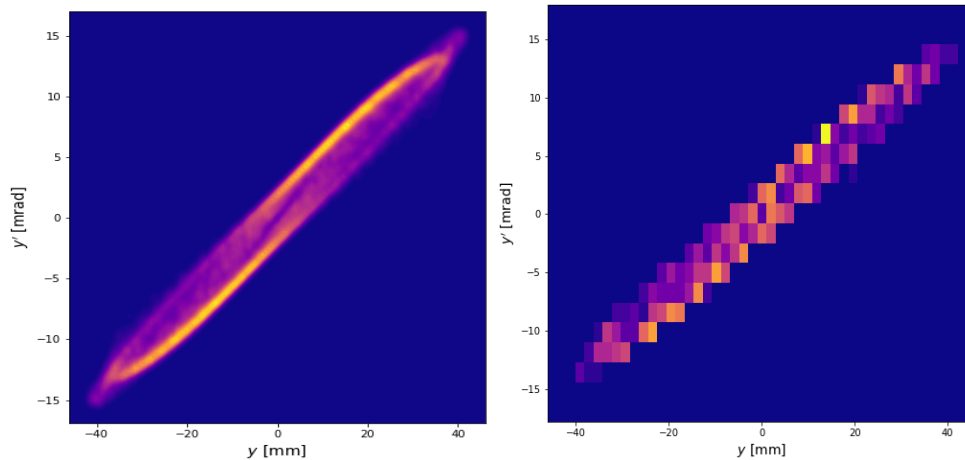


Figure 2: The phase space reconstruction shows details of the phase space beyond its emittance and Twiss parameters, such as the “hooks” seen in this distribution, indicative of nonlinear forces in the injector.

3. Errors: Estimation & Mitigation

The above COMSOL modeling effort produces a zeroth-order performance estimate for a slit-harp emittance diagnostic design. The modeling and subsequent emittance reconstruction included only sampling and binning errors but did not include positional errors associated with placement of the slit or harp, relative positional errors associated with the harp wires, space charge effects, or signal errors associated with crosstalk via secondary electron emission, electromagnetic crosstalk, and signal reflections.

3.1. Sampling and Binning Errors over Emittance Measurement Range

Sampling and binning errors arise due to the following reasons. All electrons passing through a finite slit are treated as originating from the central slit position, x_S , and electrons striking a harp wire are assigned a position x_H . Electrons that do not strike a wire are excluded from the emittance reconstruction.

To understand the magnitude of this error over a range of possible emittance values, a study was performed using a 25,000-particle electron beam whose RMS emittance was varied by uniformly scaling the phase space distribution from 10 – 100 mm-mrad in steps of 1 mm-mrad. The reconstructed emittance is compared to the true emittance over this range (figure 3). The slit-harp diagnostic design permits emittance measurements with less than 10% sampling and binning errors for $\epsilon_{y,rms}$ from 10 – 60 mm-mrad. The associated measurement reconstruction error amounts to $\sim 2.7\%$ for the original (unscaled) simulated injector beam.

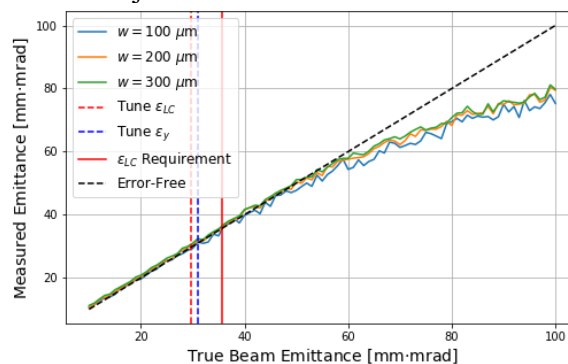


Figure 3 Emittance reconstruction results for a range of $\epsilon_{y,rms}$. Note the transition from 1:1 linear scaling to $\sqrt{\epsilon}$ scaling as the angular distribution becomes too large for the slit aspect ratio and harp extent.

3.2. Positional Errors

Positional errors arise due to several mechanisms, including shot-to-shot beam positioning jitter, actuator positioning errors, and individual harp wire positioning errors. Positional errors associated with the actuators are determined by actuator resolution and repeatability. The actuators chosen for the diagnostic have a resolution of 0.5 μm and a repeatability of 1.3 μm , and both contribute to step size errors. However, the expected beam radius (~ 40 mm) and the harp wire diameter and spacing are much larger than the actuator tolerances. Therefore, the actuator position errors are expected to be negligible.

Manufacturing tolerances for the alignment of the harp wires in the guide blocks are on the order of 35 μm . This value is greater than 10% of the wire diameter and 5% of wire spacing, and thus may produce significant errors. Emittance reconstruction was performed for a set of 1,000 different harp configurations, whose displacements from nominal position were sampled from a normal distribution with a variance of $\sigma_{x,wire}^2$. The results for $\sigma_{x,wire} = 35$ μm show that an RMS error equal to the manufacturer's specified tolerance produced a relative statistical emittance error of 0.70%. This is much lower than the error associated with binning and sampling (2.7%).

3.3. Space Charge Errors

Mutual repulsion between electrons causes the beam to expand between the slit and harp [4], in addition to the intrinsic emittance expansion alone. The beam between the slit and harp was modeled as a uniform sheet beam, with current density derived from the 1.4 kA beam current and the beam size predicted by injector simulations. For the planned Scorpius aperture widths of 100 and 200 μm , the emittance measurement error is 0.84% and 1.68%, respectively. This error may be correctible during analysis if profile measurements show that the beam is reasonably uniform.

3.4. Secondary Electron Emission

Primary electrons scatter during their interaction with electrons within a harp wire. Any secondary electron having enough energy to escape a harp wire contributes to the error associated with the signal on that wire. Additionally, crosstalk occurs when a secondary electron escapes one harp wire and is captured on another. This mixing of signals between neighboring wires leads to momentum reconstruction errors.

Typical energies of secondary electrons are a few eV ($E_s < 20$ eV). Modeling suggests that the crosstalk magnitude could be up to 10% of the magnitude of the primary signal. Positively biasing the harp wires reduces crosstalk by creating a potential well around each wire. Electron trajectory simulations in this potential well indicate that secondary electron crosstalk can be suppressed to $< 1\%$ of the signal with a 600 V bias voltage.

3.5. Errors Summary

Primary The systematic reconstruction error due to sampling and binning effects is $\sim 2.7\%$. The wire placement tolerances contribute $\sim 0.7\%$ error, and space charge contributes $\sim 2\%$ error. Secondary electron emission errors can be suppressed to $\sim 1\%$. Assuming the errors are uncorrelated and normally distributed, these sources lead to a total error of about 3.4% for a beam like the simulated injector beam.

4. Material Heat Loads

Different materials were studied to understand the thermal effects on the slit and harp due to energy deposition by the beam. National Institute of Standards and Technology (NIST) ESTAR was used to estimate the deposited energy density distribution via the continuous slowing down approximation (CSDA) model. The specific heat of the material was used to calculate the temperature rise and the resulting temperature-vs-depth profile was used as the initial condition for the heat equation to find the maximum surface temperature. The results for a 2.0 MeV beam with Scorpius beam parameters show

that 2 mm of copper is enough to stop 2.0 MeV electrons and produce a temperature rise of less than 187 K within the material and a surface temperature increase of less than 18.4 K per pulse.

5. Conclusion

In conclusion, the proposed slit-harp emittance diagnostic featuring the presented design should be able to measure the injector emittance of the NNSS Scorpius linear induction accelerator to within several percent of its true value. The design of record is a slit of width w ($100 \mu\text{m} \leq w \leq 200 \mu\text{m}$) and collimation depth $d = 2\text{mm}$, and a harp of 21 $250 \mu\text{m}$ wires separated by $500 \mu\text{m}$ each. The phase space reconstruction may also show details of the distribution that carry additional information about the beam dynamics in the injector.

Acknowledgments

This paper was prepared for and presented at the 2023 JACoW International Particle Accelerator Conference in May 2023 in Venice, Italy by Mark Raphaelian, RaphaelML@nv.doe.gov: +1-915-960-2500. This work was done by Mission Support and Test Services, LLC, under Contract No. DE-NA0003624 with the U.S. Department of Energy. DOE/NV/03624—1743

References

- [1] Benjamin Cheymol. "Development of beam transverse profile and emittance monitors for the CERN LINAC4." PhD diss., Université Blaise Pascal-Clermont-Ferrand II, 2011.
- [2] W. Blokland and C. Long. "An In-Line Emittance Scanner Based on a LabVIEW Style State Machine with Sequencer", Proc. 10th Int. Conf. on Accelerator and Large Experimental Physics Control Systems (ICALPCS'10), Geneva, Switzerland, Oct. 2005, paper PO1.057-6.
- [3] M. Stockli. "Measuring and analyzing the transverse emittance of charged particle beams." In AIP conference proceedings, vol. 868, no. 1, pp. 25-62. American Institute of Physics, 2006.
- [4] F. J. Sacherer. "RMS Envelope Equations with Space Charge," in IEEE Transactions on Nuclear Science, vol. 18, no. 3, pp. 1105-1107, June 1971, doi: 10.1109/TNS.1971.4326293.